ELSEVIER

Model Aerodynamic Tests with a Wire-driven Parallel Suspension System in Low-speed Wind Tunnel

Xiao Yangwen[a], Lin Qi[a],*, Zheng Yaqing[a,b], Liang Bin[c]

[a]*Department of Aeronautics, Xiamen University, Xiamen 361005, China*

[b]*College of Mechanical Engineering and Automation, Huaqiao University, Quanzhou 362021, China*

[c]*Shenzhen Branch, China Telecom Co. Ltd, Shenzhen 518034, China*

Abstract

Owing to the advantages of wire-driven parallel manipulator, a new wire-driven parallel suspension system for airplane model in low-speed wind tunnel is constructed, and the methods to measure and calculate the aerodynamic parameters of the airplane model are studied. In detail, a static model of the wire-driven parallel suspension is analyzed, a mathematical model for describing the aerodynamic loads exerted on the scale model is constructed and a calculation method for obtaining the aerodynamic parameters of the model by measuring the tension of wires is presented. Moreover, the measurement system for wire tension and its corresponding data acquisition system are designed and built. Thereafter, the wire-driven parallel suspension system is placed in an open return circuit low-speed wind tunnel for wind tunnel tests to acquire data of each wire tension when the airplane model is at different attitudes and different wind speeds. A group of curves about the parameters for aerodynamic load exerted on the airplane model are obtained at different wind speeds after the acquired data are analyzed. The research results validate the feasibility of using a wire-driven parallel manipulator as the suspension system for low-speed wind tunnel tests.

Keywords: wire-driven parallel manipulators; low-speed wind tunnel; suspension system; aerodynamic loads; tests

1. Introduction

As a new type of parallel manipulator, the wire-driven parallel manipulator has advantageous characteristics such as simple and reconfigurable structure, large workspace, high load capacity, high load/weight ratio, easy assembly/disassembly, high modularization, low cost and high speed[1-3].

With the recent development of parallel mechanism and force control technology, a new concept has been proposed by French National Aerospace Research Center (ONERA) in the active suspension for wind tunnel tests (SACSO) project which uses wire-driven parallel manipulator as aircraft model suspension system in low-speed wind tunnel tests[3-4]. As a new soft-style suspension, the wire-driven parallel suspension system can preferably solve the contradiction be-

tween the brace stiffness and the aerodynamic interference. It is suitable for different kinds of aircraft's wind tunnel tests such as missile dynamics and flight control, because the suspension system can not only decrease interference effects, but also bring large angles of attack and sideslip of the model[5-11]. The SACSO project supported by ONERA has been carried out for more than eight years. The research results have been applied to vertical wind tunnel tests with wind speed at 35 m/s for conceptual design of fighter. However there is nothing related to measurement of dynamic derivatives in the open literature about SACSO project[4,12-15].

We have investigated wire-driven parallel suspension system for many years and have obtained some results[16-17]: the design of the mechanisms, studies on attitude control of the model, and kinematic calibration. Besides, a prototype wire-driven parallel suspension system with eight wires has been built up to achieve the model's six degrees of freedom (6-DOF) motion control and single-DOF oscillation control. In this article, a measuring system is installed upon the prototype to detect the wires' tensions, and then the suspension

system is placed in an open return circuit low-speed wind tunnel for tests. According to the data of each wire tension, a method to calculate the aerodynamic parameters of the model is given, and the curves of model's aerodynamic parameters are obtained. The research results show that, the wire-driven parallel suspension system can be used in low-speed wind tunnel tests, and the method to calculate the model's aerodynamic parameters by measuring the wire tension is feasible.

2. Wire-driven Parallel Suspension System and its Structural Parameters

As shown in Fig.1, the suspension for wind tunnel test in this article is a 6-DOF wire-driven parallel suspension system with eight wires (WDPSS-8). The mechanism theory and the robot technology are applied to the design of the prototype and motion control of the model.

Fig.1   Prototype of WDPSS-8.

The structural parameters of WDPSS-8 prototype are shown in Fig.2. For the convenience of expression, the model plane is simplified as a cross, and the intersection point P is regarded as the origin point of the moving coordinate system $(Px_Py_Pz_P)$. The model can rotate around the point P. Then the pose of the model plane referenced to the fixed coordinate system $(OXYZ)$ can be expressed by $X = [X_P \ X_{ang}]^T$, where X_P is the position vector of point P, X_{ang} is the attitude vector of the model, which includes the roll angle γ_P (rotation around OX axis positive direction), the pitch angle α_P (rotation around OY axis positive direction) and the yaw angle β_P (rotation around OZ axis positive direction). The dimensions of the prototype are determined by the size of a certain open return circuit low-speed wind tunnel. The positions of point-shaped joints on the prototype are also confirmed. Therefore, the point-shaped joints, $B_i(i = 1,2,\cdots,8)$, in the fixed coordinate system can be expressed as $B_1(B_2)$：(0,0,0), $B_3(B_4)$: (0,0,1 060), $B_5(B_6)$: (0,–410,530), $B_7(B_8)$: (0, 410,530).
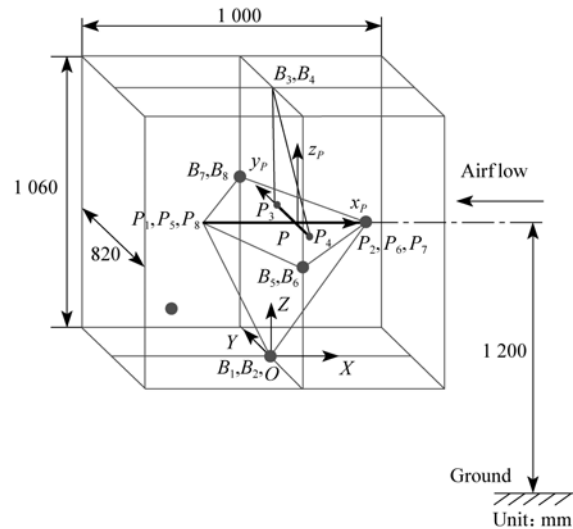

Fig.2   Structural parameters of WDPSS-8.

The positions of the connection points $P_i(i=1,2,\cdots,8)$ between wires and model in the moving coordinate system are $P_1(P_5,P_8)$: (–150,0,0), $P_2(P_6,P_7)$: (120,0,0), P_3: (0, 142.5,0), P_4: (0,–142.5,0). The values of the connection points are related to the dimensions of the model plane.

In Ref.[16], the feasibility of 6-DOF wire-driven parallel suspension system is theoretically analyzed, the control platform has been built up, and various motion controls of the model such as single-DOF rotation, combinational DOF rotation, free flight, single-DOF dynamic derivative tests have been implemented. The achievements in Ref.[16] pave the way to adjust and determine the pose of the model plane conveniently which will be discussed in the next sections.

3. Mathematical Modeling of Aerodynamic Parameters

3.1. Static model

To obtain the model's aerodynamic parameters is the main purpose in wind tunnel tests. In this article, the model's aerodynamic parameters are calculated through different aerodynamic loads before and during wind tunnel tests. Thus, the aerodynamic parameters can be calculated by measuring the driving wires' tensions.

Tension is the only force acting upon the wire and its direction is always along the wire. The model's pose and motion are controlled by changing the wires' length. It means that when the model's attitude changes,

the wires' directions and tensions also change. So, it is necessary to determine the wires' direction at any attitude of the model. To solve this problem, the relationship between the wires' length and the relative spatial position of the model is calculated first.

As shown in Fig.3, let $L_i = \overline{B_i P_i} = P_i - B_i$ ($i=1,2, \cdots, 8$), then the length of each wire can be denoted by $l_i = \|L_i\| = \|P_i - B_i\|$ ($i=1,2,\cdots, 8$), and the unit vector of L_i is denoted by $u_i = L_i/l_i$, ($i=1,2, \cdots, 8$). According to the inverse kinematic models, if the pose (X) of the model is known, the position vector of the connection points P_i, $X_{Pi}=[X_{Pi} \quad Y_{Pi} \quad Z_{Pi}]^T$, ($i=1,2, \cdots, 8$), can be given in the static coordinate system *OXYZ* by[16]

$$X_{Pi} = \begin{bmatrix} X_{Pi} \\ Y_{Pi} \\ Z_{Pi} \end{bmatrix} = \begin{bmatrix} X_P \\ Y_P \\ Z_P \end{bmatrix} + R \begin{bmatrix} x_{Pi} \\ y_{Pi} \\ z_{Pi} \end{bmatrix} \quad (1)$$

where R is coordinate transformation matrix. In detail, the R matrix can be shown as

$$R = R_x(\gamma_P)R_y(\alpha_P)R_z(\beta_P) \quad (2)$$

where

$$R_x(\gamma_P) = \begin{bmatrix} 1 & 0 & 0 \\ 0 & \cos\gamma_P & -\sin\gamma_P \\ 0 & \sin\gamma_P & \cos\gamma_P \end{bmatrix}$$

$$R_y(\alpha_P) = \begin{bmatrix} \cos\alpha_P & 0 & \sin\alpha_P \\ 0 & 1 & 0 \\ -\sin\alpha_P & 0 & \cos\alpha_P \end{bmatrix}$$

$$R_z(\beta_P) = \begin{bmatrix} \cos\beta_P & -\sin\beta_P & 0 \\ \sin\beta_P & \cos\beta_P & 0 \\ 0 & 0 & 1 \end{bmatrix}$$
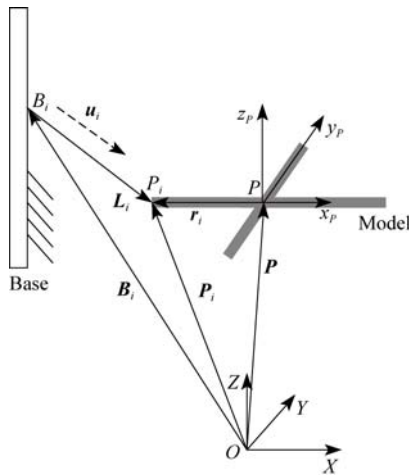

Fig.3 Kinematical notation of wire-driven parallel manipulator.

Let t_i represent each wire's force value, then the tension of each wire exerted on the model can be given by $T_i = -t_i u_i$ ($i=1,2,\cdots,8$), where the minus means the direction of T_i is contrary to that of u_i. Let $r_i = \overline{PP_i}$. When the model is in wind tunnel test, there are forces exerted on the model, such as gravity, aerodynamic forces (including lift, drag and aerodynamic moments). In order to make the model keep a certain pose, the forces of driving wires should be greater than zero.

Suppose the model is exerted by pull forces of wires, gravity and aerodynamic forces, but still keeps in balance, the statics equilibrium equation can be denoted by

$$\left. \begin{array}{l} \sum_{i=1}^{8} T_i + F_A + F_G = 0 \\ \sum_{i=1}^{8} M_i + M_A = 0 \end{array} \right\} \quad (3)$$

where F_A and M_A are the aerodynamic force and the aerodynamic moment exerting on the model respectively, F_G is the model's weight, T_i and M_i are the *i*th wire's tension and the moment exerting on the model by the wire.

Moreover, T_i and M_i can be denoted respectively by

$$\sum_{i=1}^{8} T_i = \sum_{i=1}^{8} (-t_i u_i) \quad (4)$$

$$\sum_{i=1}^{8} M_i = \sum_{i=1}^{8} (r_i \times T_i) = \sum_{i=1}^{8} r_i \times (-t_i u_i) = \sum_{i=1}^{8} (t_i u_i) \times r_i \quad (5)$$

Let $T = [T_1 \ T_1 \cdots T_8]^T$ represent the matrix of wires' tensions, $W_R = [F_R \ M_R]^T$ represent the wrench. Then W_R can be given by

$$W_R = J^T T \quad (6)$$

In Eq.(6), the values of T_i ($i=1,2,\cdots, 8$), denoted as t_i ($i=1,2,\cdots,8$), can be measured by eight force sensors directly, and J^T is the Jacobian matrix expressed as

$$J^T = \begin{bmatrix} -u_i \\ u_i \times r_i \end{bmatrix} \quad (7)$$

J^T varies as the attitude of the model changes.

3.2. Calculation of aerodynamic parameters

Wind tunnel is crucial equipment for the development of aeronautics and astronautics. Wind tunnel test is an indispensable step in the research and development of aircraft in that it is an effective way to obtain aircraft's aerodynamic parameters. The wind tunnel tests in this article are performed by placing the WDPSS-8 in an open return circuit low-speed wind tunnel. The aerodynamic forces can be obtained based on the change of wires' tensions before and during the wind tunnel test.

For convenience, subscripts "0" and "W" in this article represent the parameters before and during wind tunnel test, and subscript "A" represents the aerodynamic parameters.

Before the wind tunnel test, the model is in a balancing state with the action of gravity and wires' tensions[17-18]. Then, according to Eq.(3), the static equilibrium equation can be given by

$$\left.\begin{aligned}\sum_{i=1}^{8}\boldsymbol{T}_{i,0}+\boldsymbol{F}_{\mathrm{G}}=\boldsymbol{0}\\\sum_{i=1}^{8}\boldsymbol{M}_{i,0}=\boldsymbol{0}\end{aligned}\right\}\quad(8)$$

where $\boldsymbol{T}_{i,0}$ ($i=1,2,\cdots,8$) and $\boldsymbol{M}_{i,0}$ ($i=1,2,\cdots,8$) are the spatial force system and the spatial moment system of the eight driving wires before test respectively.

During wind tunnel test, the model is exerted by the aerodynamic force besides the gravity and the wires' tensions. However, the model is still in a balancing state. At this time, the statics equilibrium equation can be given by

$$\left.\begin{aligned}\sum_{i=1}^{8}\boldsymbol{T}_{i,\mathrm{W}}+\boldsymbol{F}_{\mathrm{A,W}}+\boldsymbol{F}_{\mathrm{G}}=\boldsymbol{0}\\\sum_{i=1}^{8}\boldsymbol{M}_{i,\mathrm{W}}+\boldsymbol{M}_{\mathrm{A,W}}=\boldsymbol{0}\end{aligned}\right\}\quad(9)$$

where $\boldsymbol{T}_{i,\mathrm{W}}$ ($i=1,2,\cdots,8$) and $\boldsymbol{M}_{i,\mathrm{W}}$ ($i=1,2,\cdots,8$) respectively express the spatial force system and moment system of the driving wires, and $\boldsymbol{F}_{\mathrm{A,W}}$ and $\boldsymbol{M}_{\mathrm{A,W}}$ respectively express the aerodynamic forces and moments acting on the model by the blowing.

Based on Eq.(6), Eqs.(8)-(9) can be expressed in matrix as

$$\boldsymbol{W}_{\mathrm{R,0}}=\boldsymbol{J}^{\mathrm{T}}\boldsymbol{T}_{0}=\boldsymbol{0}-\begin{bmatrix}\boldsymbol{F}_{\mathrm{G}}\\\boldsymbol{0}\end{bmatrix}\quad(10)$$

$$\boldsymbol{W}_{\mathrm{R,W}}=\boldsymbol{J}^{\mathrm{T}}\boldsymbol{T}_{\mathrm{W}}=-\begin{bmatrix}\boldsymbol{F}_{\mathrm{A,W}}\\\boldsymbol{M}_{\mathrm{A,W}}\end{bmatrix}-\begin{bmatrix}\boldsymbol{F}_{\mathrm{G}}\\\boldsymbol{0}\end{bmatrix}\quad(11)$$

Then the aerodynamic forces can be calculated by subtracting Eq.(11) from Eq.(10):

$$\begin{bmatrix}\boldsymbol{F}_{\mathrm{A,W}}\\\boldsymbol{M}_{\mathrm{A,W}}\end{bmatrix}=\boldsymbol{J}^{\mathrm{T}}(\boldsymbol{T}_{0}-\boldsymbol{T}_{\mathrm{W}})=$$
$$\begin{bmatrix}F_{X}&F_{Y}&F_{Z}&M_{X}&M_{Y}&M_{Z}\end{bmatrix}^{\mathrm{T}}\quad(12)$$

where F_{X} is drag, F_{Y} sideslip force, F_{Z} lift, M_{X} roll moment, M_{Y} pitch moment, and M_{Z} yaw moment.

According to the aerodynamics, the aerodynamic parameters can be determined by

$$\left.\begin{aligned}C_{Z}=2F_{Z}/(\rho v^{2}S)\\C_{X}=2F_{X}/(\rho v^{2}S)\end{aligned}\right\}\quad(13)$$

$$K=\frac{C_{Z}}{C_{X}}\quad(14)$$

where C_{Z} and C_{X} respectively stand for the lift coefficient and drag coefficient of the model, K is the lift-drag ratio, ρ the density of airflow, v the velocity of airflow, and S the reference area of the model[19].

3.3. Brief description of force-measurement system

The force-measurement system shown in Fig.4 is composed of power, force sensors, transducers, interface circuit and data acquisition card.
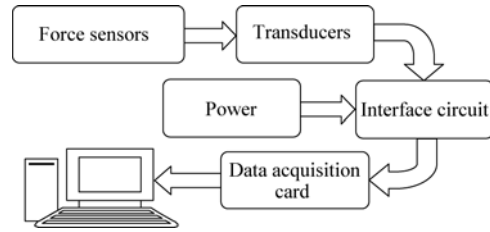

Fig.4　Block diagram of data-acquisition module of force-measurement system.

The power makes sure that the sensors, transducers and interface circuit could work steadily under the 12 V direct current. The changes of tensions are measured by sensors and transmitted to the transducers. After the signals are regulated and patched into corresponding channels, the analog signals are converted into digital data, then acquired by the data acquisition card and transmitted into the control computer for further processing[20].

4. Wind Tunnel Tests and Results

4.1. Wind tunnel and airplane model

As shown in Fig.5, the model is suspended by WDPSS-8 in the open return circuit low-speed wind tunnel for tests. The size of the tunnel cross section is 520 mm × 420 mm, and the airflow speed can be adjusted among 0-50 m/s.

Fig.5　WDPSS-8 suspension system in wind tunnel.

Because the main purpose of the study is to verify the feasibility, advantages and disadvantages of the method of using WDPSS-8 in wind tunnel tests to obtain the model's aerodynamic parameters, instead of discussing the aerodynamic performance of the model, the plane model can be designed as simply as possible. Therefore the actual model is not a standard scaled model as designed in Fig.6. The body of the model in Fig.6 is designed as 270 mm long and 285 mm wide in the wing span. For the convenience of measurement,

the model is divided into two parts and is made hollow in order to place the sensor and other units. The model is designed in the SolidWorks environment and manufactured with the help of rapid prototyping system HRPL-II.
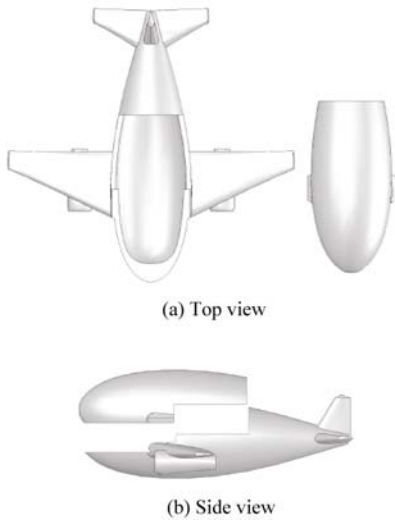

(a) Top view

(b) Side view

Fig.6   Structural sketch of airplane model.

4.2. Results of wind tunnel tests

The tests have been conducted at different wind speeds by setting the model at different pitch or yaw angles in the wind tunnel respectively. The eight wires' tensions in all test conditions are measured and the experimental data are acquired and processed. Therefore, the aerodynamic loads exerting on the model can be calculated with the acquired data according to Eqs.(8)-(12).

(1) Variation of wires' tensions

As shown in Fig.5, to observe the variation of eight wires' tensions, the model is at tests under the conditions of three wind speeds, i.e. 17.25 m/s (Flow 1), 25.51 m/s (Flow 2), and 41.42 m/s (Flow 3). The variations of wires' tensions are shown in Figs.7-8 in which the pitch angle of the model is set at 0° and 15°, respectively.
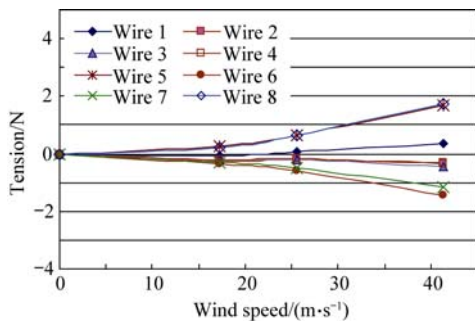

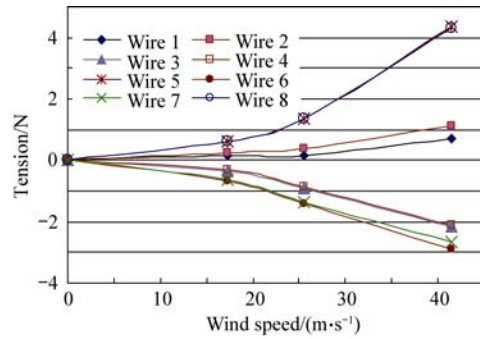Fig.7   Tension of each wire in blowing ($\alpha_P = \beta_P = \gamma_P = 0°$).

Fig.8   Tension of each wire in blowing ($\alpha_P = 15°$, $\beta_P = \gamma_P = 0°$).

The values given in Figs.7-8 are the differences of wires' tensions before and during the tests. They show that the wires' tensions rise as the wind speed increases. It can also be seen from Fig.7 that the variation tendencies of each two wires are symmetric, when the model is in the zero pose ($\alpha_P = \beta_P = \gamma_P = 0°$). This character is consistent with symmetric configuration of WDPSS-8. However, the variations will not be symmetric any more when the attitude of the model is changed. In this case, the tensions of the wires controlling the pose of the model increase or decrease.

(2) Curves of aerodynamic coefficients

The aerodynamic parameters including the drag, sideslip, lift and the moments acting on the model can be calculated in accordance with Eqs.(8)-(12) with the acquired test data. Aerodynamic coefficients, which include coefficients of lift, drag and lift-drag ratio, can also be obtained conveniently according to Eqs.(13)-(14). The changes of the aerodynamic coefficients vary with the changes of attitude.

The variation curves of aerodynamic coefficients are shown in Figs.9-11 when the model is at different pitch angles at three different wind speeds mentioned above.
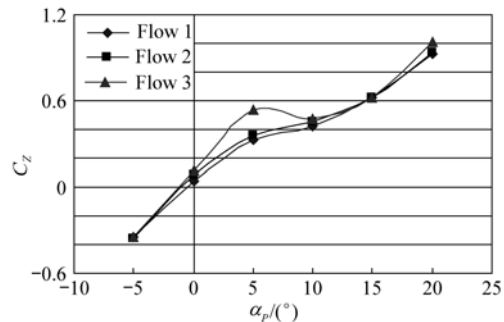

Fig.9 C_Z curves for pitching lift coefficient ($\beta_P = \gamma_P = 0°$).

There are no aerodynamic coefficient data in literature for reference, because the model used is not a standard scale model. But, it can still be concluded that the variation trends shown in Figs.9-11 are reasonable. The figures also show that when the self-designed model is at zero pose, the drag is at the lowest point;
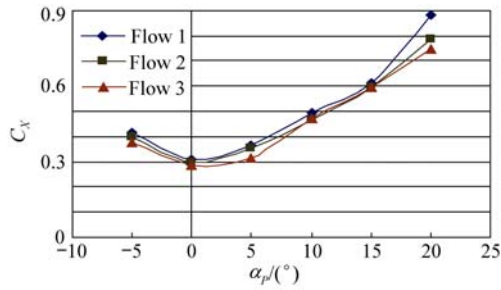
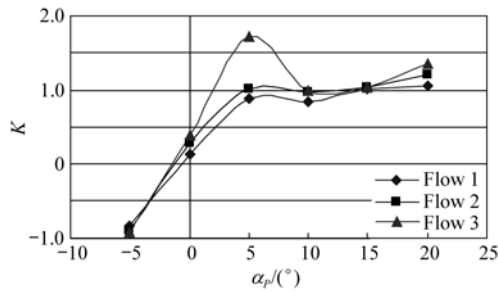Fig.10 C_X curves for pitching drag coefficient ($\beta_P = \gamma_P = 0°$).

Fig.11 K curves for pitching lift-drag ratio ($\beta_P = \gamma_P = 0°$).

when the model's pitch angle is near 5°, the lift-drag ratios are higher with better aerodynamic performance.

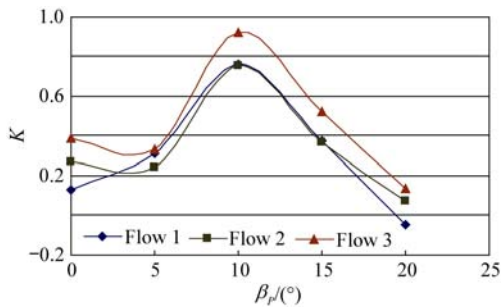The lift-drag ratios are shown in Fig.12 when the model is at different yaw angles and wind speeds.

Fig.12 K curves for yawing lift-drag ratio ($\alpha_P = \gamma_P = 0°$).

The aerodynamic moment data are also acquired by changing the attitudes of the model and wind speeds through wind tunnel tests.

The curves of aerodynamic moments varying with wind speed are shown in Fig.13 ($\alpha_P = \gamma_P = \beta_P = 0°$). In theory, due to the model's symmetry, the roll moment M_X and yaw moment M_Z should both equal zero. But the measured moments are not zero as shown in Fig.13. It is probably because the model is not aligned to the airflow. After all, the prototype is still at the starting stage, and the research on the measurement of model's attitude is immature in terms of measuring accuracy. The pitch moment M_Y appears to be nose-down moment, which is probably related to the configuration of the model. Nevertheless, the results are reasonable.
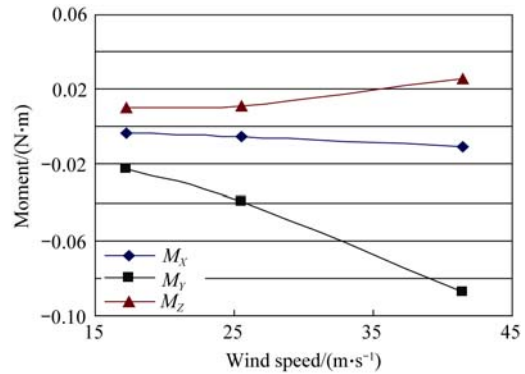

Fig.13   Aerodynamic moments vs wind speed.

(3) Curves of aerodynamic moments

The variations of aerodynamic moments are also obtained in the wind tunnel tests by setting the model at different attitudes and blowing speeds.

Fig.14 shows the influence of pitch angle α_P on the pitch moment at different airflow speeds. The values of pitch moments are close to zero when the pitch angle α_P is between 5° and 10° rather than at 0°. Such results are probably caused by the non-standard design of the model plane. When the pitch angle α_P is less than 5°, the model is subjected to nose-down moments and when the pitch angle α_P is much larger, it is subjected to nose-up moments. The facts prove that the results accord with the physical meaning.
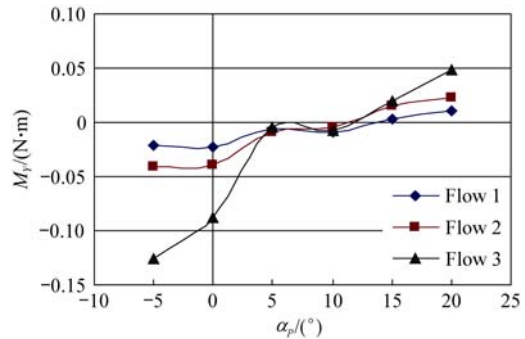

Fig.14   Pitch moment M_Y vs pitch angle α_P ($\beta_P = \gamma_P = 0°$).

The aerodynamic moments (including pitch moment M_Y, yaw moment M_Z and roll moment M_X) varying with the yaw angles are also shown in Figs.15-17. The
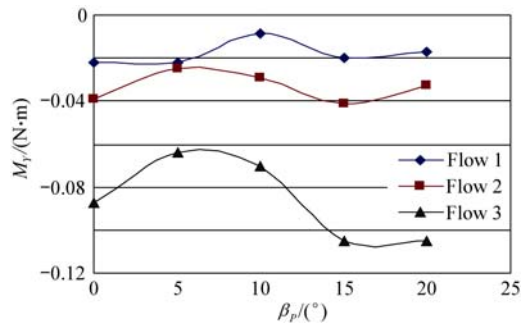

Fig.15   Pitch moment M_Y vs yaw angle β_P ($\alpha_P = \gamma_P = 0°$).
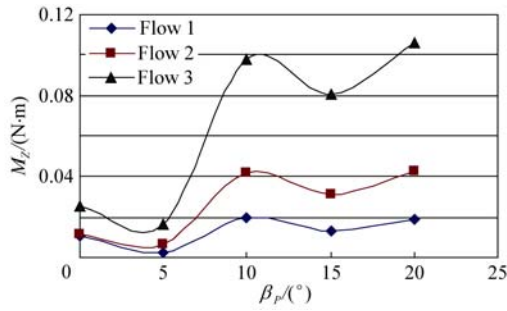
Fig.16   Yaw moment M_Z vs yaw angle β_P ($\alpha_P = \gamma_P = 0°$).
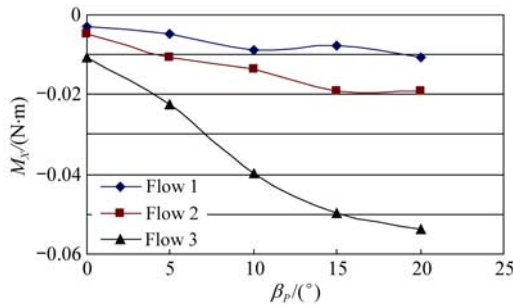

Fig.17   Roll moment M_X vs yaw angle β_P ($\alpha_P = \gamma_P = 0°$).

variations of the moments are not only related to the model's attitude and the airflow speed, but also influenced by the model's configuration.

5. Conclusions

(1) A type of suspension for wind tunnel test is proposed and the prototype of wire-driven parallel suspension system (WDPSS-8) is built up. The analysis of the static model is applied to the WDPSS-8. In order to obtain the aerodynamic parameters, a system of measuring wires' tensions including the data collection and processing is constructed. The mathematical model of the test system is built. A method of calculating model's aerodynamic parameters by experimental data is presented.

(2) The WDPSS-8 is placed in an open return circuit low-speed wind tunnel for tests. According to the measured wires' tensions, the variations of aerodynamic parameters with pose angle and airflow speed are presented. The results are analyzed.

(3) The study in this article is still at the exploring stage, and none of the related authoritative data can be compared with the results obtained at present, for the model used in tests is non-standard. However, the test results' reasonability has validated the feasibility of using a wire-driven parallel manipulator as the suspension system for low-speed wind tunnels.

References

[1]   Bosscher P, Ebert-Uphoff I. Wrench-based analysis of cable-driven robots. IEEE Proceedings International Conference on Robotics and Automation 2004; 4950-4955.

[2]   Zheng Y Q, Lin Q, Liu X W. Design methodology of wire-driven parallel support systems in the low speed wind tunnels and attitude control scheme of the scale model. Acta Aeronautica et Astronautica Sinica 2005; 26(6): 774-778. [in Chinese]

[3]   Liu X W, Zheng Y Q, Lin Q. Overview of wire-driven parallel kinematic manipulators for aircraft wind tunnels. Acta Aeronautica et Astronautica Sinica 2004; 25(4): 393-400.[in Chinese]

[4]   Lafourcade P, Llibre M, Reboulet C. Design of a parallel wire-driven manipulator for wind tunnels. Proceedings of the Workshop on Fundamental Issues and Future Directions for Parallel Mechanisms and Manipulators. 2002; 187-194.

[5]   Roos F W. Micro blowing for high-angle-of-attack vortex flow control on fighter aircraft. Journal of Aircraft   2001; 38(3): 454-457.

[6]   Bernhardt J E, Williams D R. Close-loop control of forebody flow asymmetry. Journal of Aircraft 2000; 37(3): 491-498.

[7]   Wu C. Wire suspension system for wind tunnel dynamic testing. International Aviation 2004(5): 62. [in Chinese]

[8]   Gu Y S, Ming X. Forebody vortices control using a fast swirging micro tip-strake at high angles of attack. Acta Aeronautica et Astronautica Sinica 2003; 24(2): 102-106.[in Chinese]

[9]   Bennett R M, Farmer M G, Mohr R L, et al. Wind-tunnel technique for determining stability derivatives from cable-mounted models. Journal of Aircraft 1978; 15(5): 304-310.

[10]   Griffin S A. Vane support system(VSS), a new generation wind tunnel model support system. AIAA-1991-398, 1991.

[11]   Erickson G E. High angle-of-attack aerodynamics. Annual Review of Fluid Mechanics 1995(27): 45-88.

[12]   Lafourcade P, Llibre M, Reboulet C. Le manipulateur à câbles SACSO. Conférence Internationale Francophone d'Automatique. 2002; 8-10. [in French]

[13]   Lafourcade P, Llibre M. First steps toward a sketch-based design methodology for wire-driven manipulators. IEEE/ASME International Conference on Advanced Intelligent Mechatronics. 2003; 20-24.

[14]   Lafourcade P. Etude de manipulateurs parallèles à câbles, conception d'une suspension active pour soufflerie. thèse de docteur ingénieur de l'ENSAE. 2004. [in French]

[15]   Farcy D, Llibre M, Carton P, et al. SACSO: wire-driven parallel set-up for dynamic tests in wind tunnel-review of principles and advantages for identification of aerodynamic models for flight mechanics. 8th ONERA-DLR Aerospace Symposium. 2007.

[16]   Lin Q, Liang B, Zheng Y Q. Control study on model attitude and oscillation by wire-driven parallel manipulator support system for low-speed wind tunnel. Journal of Experiments in Fluid Mechanics 2008; 22(3): 75-79. [in Chinese]

[17]   Zheng Y Q, Lin Q, Liu X W, et al. On wire-driven parallel suspension systems for static and dynamic derivatives of the aircraft in low-speed wind tunnels. Acta Aeronautica et Astronautica Sinica 2009; 30(8)：1549-1554. [in Chinese]

[18]   Liu X, Qiu Y Y, Sheng Y. Stiffness enhancement and motion control of a 6-DOF wire-driven parallel

manipulator with redundant actuations for wind tunnels. Acta Aeronautica et Astronautica Sinica 2009; 30(6): 1156-1164. [in Chinese]

[19] Klein V. Estimation of aircraft aerodynamic parameters from flight data. Progress in Aerospace Sciences 1989; 26(1): 1-77.

[20] Li Y, Ding X Z, Wang Y K. Force measurement system of a low-speed wind tunnel. The Ninth International Conference on Electronic Measurement & Instruments. 2009; 302-305.

Biographies:

Xiao Yangwen Born in 1984, he received B.S. and M.S. degrees from Xiamen University in 2006 and 2009 respectively, and now works in Aviation Motor Control System Institute, Aviation Industry Corporation of China. His major is flight vehicle propulsion engineering. His main academic interest is mechanical and electrical integration.
E-mail: awenxyw@163.com

Lin Qi Born in 1954, she received B.S., M.S. and Ph.D. degrees from Nanjing University of Aeronautics and Astronautics in 1982, 1984 and 1988 respectively and is currently a professor of Xiamen University. Her main research fields are gas dynamics, aviation engineering and mechanical & electrical integration.
E-mail: qilin@xmu.edu.cn

Zheng Yaqing Born in 1974, she received B.S. and M.S. degrees from Fuzhou University in 1996 and 1999 respectively, and Ph.D. degree from Huaqiao University in 2005. Currently, she is an associate professor in Huaqiao University and a postdoctoral fellow in Xiamen University. Her main research interests include wire-driven parallel manipulators and differential flatness-based robotic systems.
E-mail: yq_zheng@hqu.edu.cn